



HAL
open science

Inverse Scattering for Soft Fault Diagnosis in Electric Transmission Lines

Qinghua Zhang, Michel Sorine, Mehdi Admane

► **To cite this version:**

Qinghua Zhang, Michel Sorine, Mehdi Admane. Inverse Scattering for Soft Fault Diagnosis in Electric Transmission Lines. 2009. inria-00365991v1

HAL Id: inria-00365991

<https://inria.hal.science/inria-00365991v1>

Submitted on 5 Mar 2009 (v1), last revised 26 May 2010 (v2)

HAL is a multi-disciplinary open access archive for the deposit and dissemination of scientific research documents, whether they are published or not. The documents may come from teaching and research institutions in France or abroad, or from public or private research centers.

L'archive ouverte pluridisciplinaire **HAL**, est destinée au dépôt et à la diffusion de documents scientifiques de niveau recherche, publiés ou non, émanant des établissements d'enseignement et de recherche français ou étrangers, des laboratoires publics ou privés.

Inverse Scattering for Soft Fault Diagnosis in Electric Transmission Lines

Qinghua Zhang, Michel Sorine and Mehdi Admane

Abstract—Today’s advanced reflectometry methods provide an efficient solution for the diagnosis of hard faults (open and short circuits) in electric transmission lines, but they are much less efficient for soft faults (spatially smooth variations of characteristic impedance). This paper completes an important missing piece for the application of the inverse scattering transform to the diagnosis of soft faults in electric transmission lines, by clarifying the relationship between the reflection coefficient measured with reflectometry instruments and the mathematical object of the same name used in the inverse scattering transform. The feasibility of this approach is then demonstrated by numerical simulation of lossless transmission lines affected by soft faults, and by the solution of the inverse scattering problem effectively retrieving smoothly varying characteristic impedance profiles from reflection coefficients.

I. INTRODUCTION

The fast development of electronic devices in modern engineering systems and in consumer products comes with an increasing number of electric wires in these equipments, and also inevitably with more and more failures related to electric connections. This fact has motivated research projects on methods for the diagnosis of faults in electric transmission lines. In this context, the technology of reflectometry has been extensively studied by different research groups [1], [2]. It consists in injecting electric signals from one end or from both ends of a line and in analyzing the reflected electric waves. At least in laboratory tests, currently this technology is able to detect and to locate hard faults (open circuit or short circuit) up to an accuracy of about 10 cm. For soft faults, however, no similar result has been reported, to our knowledge. In a recent publication [3], the difficulty for detecting frays using existing reflectometry methods has been analyzed. These investigated frays are various degradations resulting in *piecewise constant* characteristic impedance profiles. The difficulty is due to the weakness of the reflections caused by the discontinuities at the borders of fray segments.

In this paper, the considered soft faults are modeled as *spatially smooth variations of characteristic impedance*. By making experiments at one end or at both ends of a transmission line, it is obviously difficult to inspect such soft faults. Nevertheless, there have been theoretical studies in this direction, based on the *inverse scattering* transform. By formulating the inverse scattering problem for both lossless and lossy transmission lines, Jaulent’s pioneer work [4] has founded the theoretic basis for inspecting distributed

characteristics of transmission lines from reflectometry measurements. Despite this theoretic result of a quarter of a century ago, there has been an important gap to fill before its practical application.

This paper constitutes an attempt to fill the gap between the inverse scattering transform and its application to electric transmission line fault diagnosis. The relation between the reflection coefficient (measured with a network analyzer or reflectometry instruments) and the scattering data (the start point of the inverse scattering transform) will be clearly established. The feasibility of this approach will be illustrated by numerical simulations of lossless transmission lines with smooth variations of characteristic impedances, and by the solution of the inverse scattering problem, which effectively retrieves the characteristic variations of the simulated transmission lines.

Only *lossless* transmission lines are considered in this paper. Though the theoretic result of [4] covers both lossless and lossy lines, the numerical implementation of the inverse scattering transform is more difficult in the lossy case. This difficulty will be explained in the conclusion section.

The characteristic impedance of the considered transmission line is assumed twice differentiable with respect to the space variable along the longitudinal axis of the line. It is also assumed that the characteristic impedance profile is sufficiently regular so that the resonance modes of the transmission line, if any, can be neglected. This assumption will be more clearly explained in the section about mathematical modeling of transmission lines. From the practical point of view, it is a “softness” assumption of the faults affecting the characteristic impedance, excluding hard faults that can be well addressed with today’s mature reflectometry methods.

To complete the list of assumptions, the values of the characteristic impedance at the two ends of the considered transmission line are assumed known.

This paper is organized as follows. Section II is about the formulation of the inverse scattering problem applied to the monitoring of transmission line characteristic impedance, with, in particular, Section II-C clarifying the relationship between the reflection coefficient measured with reflectometry instruments and the mathematical object of the same name used in the inverse scattering transform. Simulation results are presented in Section III. Concluding remarks are made in Section IV.

II. TRANSMISSION LINE AND INVERSE SCATTERING

The purpose of this section is to present the transformations of the telegrapher’s equations leading to the Zakharov-Shabat equations and the related inverse scattering problem.

This work has been supported by the ANR SEEDS project (Smart Embedded Electronic Diagnosis Systems).

Q.Z. and M.S. are with INRIA, Domaine de Voluceau-Rocquencourt, 78153 Le Chesnay Cedex, France. Q.Z. is also with IRISA, Campus de Beaulieu, 35042 Rennes, France. M.A. was with INRIA during his work on this project. Emails: zhang@irisa.fr, Michel.Sorine@inria.fr.

The basic result has been established by Jaulent [4], but there has been an important missing piece: the connection between the practically measured *reflection coefficient* and the mathematical object of the same name (also referred to as *scattering data*) used in the solution of the inverse scattering problem. It will be shown that the two reflection coefficients, originally defined in different contexts, do coincide, up to a negative sign.

A. From telegrapher's equations to Zakharov-Shabat equations

The telegrapher's equations are a widely used model of electric transmission lines for most engineering purposes. For a lossless transmission line, let $L(z)$ and $C(z)$ be respectively the distributed inductance and capacitance along the longitudinal axis z of the line. The telegrapher's equations, in their harmonic form, then write

$$\frac{\partial}{\partial z} V(k, z) - jkL(z)I(k, z) = 0 \quad (1a)$$

$$\frac{\partial}{\partial z} I(k, z) - jkC(z)V(k, z) = 0 \quad (1b)$$

where j is the imaginary unit, k is the frequency (it will play the role of wave number after the Liouville transformation), V and I are the voltage and the current, both being functions of k and z .

To connect these equations to the inverse scattering transform, the first step is to apply a coordinate change defined by the Liouville transformation

$$x(z) = \int_0^z \sqrt{L(s)C(s)} ds \quad (2)$$

The physical meaning of the variable $x(z)$ is the wave propagation time from the position 0 to the position z . It is also referred to as *electric distance*.

After the coordinate change from z to x , by abuse of notation, $L(z(x))$ will be simply written as $L(x)$, and similarly for $C(x)$, $V(k, x)$, $I(k, x)$.

In the new coordinate system, define two new variables

$$\nu_1(k, x) = \frac{1}{\sqrt{2}} \left(Z_0^{\frac{1}{2}}(x)I(k, x) - Z_0^{-\frac{1}{2}}(x)V(k, x) \right) \quad (3a)$$

$$\nu_2(k, x) = \frac{1}{\sqrt{2}} \left(Z_0^{\frac{1}{2}}(x)I(k, x) + Z_0^{-\frac{1}{2}}(x)V(k, x) \right) \quad (3b)$$

with

$$Z_0(x) = \sqrt{\frac{L(x)}{C(x)}} \quad (4)$$

being the *characteristic impedance* of the lossless transmission line. Some direct computations then lead to

$$\frac{\partial \nu_1(k, x)}{\partial x} + jk\nu_1(k, x) = q(x)\nu_2(k, x) \quad (5a)$$

$$\frac{\partial \nu_2(k, x)}{\partial x} - jk\nu_2(k, x) = q(x)\nu_1(k, x) \quad (5b)$$

with

$$q(x) = \frac{1}{4} \frac{d}{dx} \left[\ln \frac{L(x)}{C(x)} \right] = \frac{1}{2Z_0(x)} \frac{d}{dx} Z_0(x) \quad (6)$$

Equations (5), known as Zakharov-Shabat equations, constitute the main mathematical object connecting the electric transmission line to the scattering theory. The related inverse scattering transform computes the so-called *potential function* $q(x)$ from the *reflection coefficient* (defined later in this paper). It is clear that the characteristic impedance along the x -axis as defined in equation (4) can be determined from this potential function $q(x)$ through the ratio $L(x)/C(x)$. Hence the inverse scattering transform provides a powerful mathematical tool for the monitoring of the characteristic impedance profile in electric transmission lines.

To retrieve the potential function $q(x)$ (and thus the characteristic impedance $Z_0(x)$) from the reflection coefficient only, it is required that the Zakharov-Shabat equations (5) have no bound state (spatially localized solution). Physically, this assumption means that the transmission line has no resonance mode. In practice the method presented in this paper tolerates weak resonance modes, which can be ensured by assuming a sufficiently regular characteristic impedance profile along the transmission line. This completes the "soft fault" assumption made in the introduction section.

In the following subsections, the *reflection coefficient* will be first defined through the limiting behavior of fundamental solutions of the Zakharov-Shabat equations, following a standard construction of the scattering theory. Its relationship with the reflection coefficient measured in practice with a network analyzer or with reflectometry instruments will then be clarified.

B. Fundamental solutions of the Zakharov-Shabat equations and the reflection coefficient

Assume that, for an infinitely long lossless transmission line, the characteristic impedance $Z_0(x)$ as defined in (4) tends to constant limits when $x \rightarrow \pm\infty$ (a practical interpretation of this assumption for finite length lines will be given in the next subsection). Assume further that the potential function $q(x)$ as defined in (6) decays sufficiently fast so that $x^n q(x) \rightarrow 0$ for any integer n when $x \rightarrow \pm\infty$.

Under these assumptions, for any positive value of k , the solutions of the Zakharov-Shabat equations (5) have their limiting behaviors expressed in terms of $\exp(\pm jkx)$ when $x \rightarrow \pm\infty$. Consider the solution corresponding to an incident wave emitted from the left with its limiting behaviors satisfying

$$\lim_{x \rightarrow +\infty} \nu_1(k, x) = 0 \quad (7a)$$

$$\lim_{x \rightarrow -\infty} \nu_2(k, x) \exp(-jkx) = 1 \quad (7b)$$

The left limiting behavior of this solution (known as a Jost solution) then defines the reflection coefficient $r(k)$:

$$r(k) = \lim_{x \rightarrow -\infty} \frac{\nu_1(k, x)}{\nu_2(k, x)} \exp(2jkx) \quad (8)$$

where the factor $\exp(2jkx)$ is for the purpose of demodulation so that the limit is taken for the amplitude ratio of the two waves $\nu_1(k, x)$ and $\nu_2(k, x)$. This coefficient $r(k)$ is sometimes referred to as the *left reflection coefficient*,

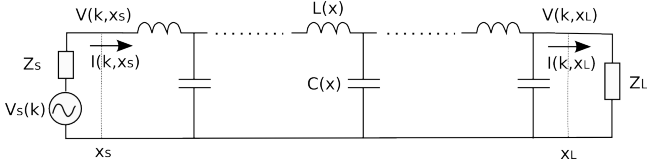


Fig. 1. A transmission line connected to a voltage source with its internal impedance $Z_s = Z_0(x_s)$ and to a matched load $Z_L = Z_0(x_L)$.

because it represents the ratio between the incident wave $\nu_2(k, x)$ coming from $-\infty$ and the reflected wave $\nu_1(k, x)$. Similarly, the right reflection coefficient is defined by symmetry.

C. practical measurement of the reflection coefficient

The reflection coefficient defined in equation (8) follows the convention usually used in the scattering theory. In practice, for electric transmission line fault diagnosis, experiments are made by injecting and measuring electric waves. It is thus of practical importance to relate the reflection coefficient $r(k)$ as defined in (8) to voltage and/or current signals. This is exactly the purpose of this subsection.

Consider a transmission line of finite length. Assume that the left end and the right end of the line correspond respectively to $x = x_s$ and $x = x_L$, with $x_s < x_L$.

Now connect the right end of the line to a matched load, that is, a load with its impedance Z_L equal to $Z_0(x_L)$. For wave propagation inside the transmission line, connecting a matched load is equivalent to extending infinitely the line with the constant characteristic impedance $Z_0(x_L)$.

To the left end of the line, connect an alternating voltage source, of frequency k . The voltage of the source is

$$V_s(k) = V_0(k) \exp(jkx_s) \quad (9)$$

with its amplitude $V_0(k)$ possibly depending on k . It is assumed that this power source has its internal impedance Z_s equal to $Z_0(x_s)$. See Figure 1 for an illustration of the transmission line and its connections. The locally matched source connected at $x = x_s$ is equivalent to an ideal voltage source $V_s(k)$ connected through an infinitely long transmission line with constant characteristic impedance $Z_0(x_s)$.

For a given transmission line with a certain characteristic impedance profile $Z_0(x)$ (for $x \in [x_s, x_L]$) connected to the voltage source $V_s(k)$ and the matched load Z_L , after the transient period, the stationary voltage and current waves along the transmission line are completely determined. As the connections made at the two ends of the line are equivalent to infinitely extending the line with the constant characteristic impedance $Z_0(x_s)$ at the left side and $Z_0(x_L)$ at the right side, virtually the voltage $V(k, x)$ and the current $I(k, x)$ are defined for all real value $x \in \mathbb{R}$. This voltage-current pair corresponds to a solution of the Zakharov-Shabat equations in $\nu_1(k, x)$ and $\nu_2(k, x)$ through the linear transformation (3). Is this a Jost solution satisfying the limiting conditions (7)?

Let us examine the value of $\nu_1(k, x)$ at $x = x_L$. Because the load $Z_L = Z_0(x_L)$ is connected at $x = x_L$,

$$V(k, x_L) = Z_L I(k, x_L) = Z_0(x_L) I(k, x_L)$$

Following (3a),

$$\begin{aligned} \nu_1(k, x_L) &= \frac{1}{\sqrt{2}} \left(Z_0^{\frac{1}{2}}(x_L) I(k, x_L) \right. \\ &\quad \left. - Z_0^{-\frac{1}{2}}(x_L) Z_0(x_L) I(k, x_L) \right) \\ &= 0 \end{aligned}$$

As virtually the transmission line is extended with the constant impedance $Z_0(x) = Z_0(x_L)$ for $x > x_L$, the potential function $q(x) = 0$ for $x > x_L$. According to (5a) with $q(x) = 0$, the value $\nu_1(k, x_L) = 0$ implies that $\nu_1(k, x) = 0$ for all $x > x_L$. Thus the first condition (7a) of Jost solution is satisfied.

To check the second condition (7b), let us examine the behavior of $\nu_2(k, x)$ at the left side. As the locally matched source connected at $x = x_s$ is equivalent to an ideal voltage source $V_s(k)$ connected through an infinitely long transmission line with constant characteristic impedance $Z_0(x_s)$, virtually $q(x) = 0$ for $x < x_s$. Let $\nu_2(k, x_s) = c(k) \exp(jkx_s)$ for some complex value $c(k)$ depending on k , then following (5b) with $q(x) = 0$,

$$\nu_2(k, x) = c(k) \exp(jkx)$$

for all $x < x_s$. It is then clear that the pair $\nu_1(k, x)$ and $\nu_2(k, x)$ is a Jost solution, up to the factor $c(k)$. This factor does not matter in the definition of the reflection coefficient $r(k)$ given in (8), as $\nu_1(k, x)$ and $\nu_2(k, x)$ could be both divided by $c(k)$.

Again as virtually $q(x) = 0$ for all $x < x_s$, it is easy to check that, for all $x < x_s$,

$$\frac{\nu_1(k, x)}{\nu_2(k, x)} \exp(2jkx) = \frac{\nu_1(k, x_s)}{\nu_2(k, x_s)} \exp(2jkx_s) \quad (10)$$

The limit in the theoretic definition (8) of the reflection coefficient can then be replaced by

$$r(k) = \frac{\nu_1(k, x_s)}{\nu_2(k, x_s)} \exp(2jkx_s) \quad (11)$$

Following Figure 1, by Ohm's law,

$$I(k, x_s) = \frac{V_s(k) - V(k, x_s)}{Z_s} = \frac{V_s(k) - V(k, x_s)}{Z_0(x_s)} \quad (12)$$

By substituting $I(k, x_s)$ with (12) in the definition (3) of $\nu_1(k, x)$ and $\nu_2(k, x)$, a few lines of computation lead to

$$\frac{\nu_1(k, x_s)}{\nu_2(k, x_s)} = \frac{V_s(k) - 2V(k, x_s)}{V_s(k)} \quad (13)$$

A combination of equations (11) and (13) then yields

$$V(k, x_s) = \frac{1}{2} V_s(k) - \frac{1}{2} V_s(k) r(k) \exp(-2jkx_s)$$

Remind that $V_s(k) = V_0(k) \exp(jkx_s)$ as assumed in (9), the last equation then becomes

$$\begin{aligned} V(k, x_s) &= \frac{1}{2} V_0(k) \exp(jkx_s) - \frac{1}{2} V_0(k) r(k) \exp(-jkx_s) \\ &= V_i(k) \exp(jkx_s) + V_r(k) \exp(-jkx_s) \end{aligned}$$

with the demodulated incident wave $V_i(k)$ and reflected wave $V_r(k)$ defined as

$$V_i(k) = \frac{1}{2}V_0(k) \quad (14a)$$

$$V_r(k) = -\frac{1}{2}V_0(k)r(k) \quad (14b)$$

The usually defined reflection coefficient is

$$\frac{V_r(k)}{V_i(k)} = -r(k) \quad (15)$$

which is in agreement with the reflection coefficient $r(k)$ defined in (11), up to the difference of sign.

In practice, $V(k, x_s)$ can be measured by a voltmeter. Its incident wave component $V_i(k)$ is known from the voltage source, and its reflected wave component can then be easily deduced. The reflection coefficient is then readily computed. This experience is repeated with different values of k , covering a sufficiently large spectrum.

D. Inverse scattering for characteristic impedance monitoring

The inverse scattering transform consists of the following steps for computing the potential function $q(x)$, and thus the profile of $L(x)/C(x) = Z_0^2(x)$, from the reflection coefficient $r(k)$. See [5] for details.

- 1) Let the Fourier transform of the reflection coefficient $r(k)$ be

$$\rho(x) = \frac{1}{2\pi} \int_{-\infty}^{+\infty} r(k) \exp(-jkx) dk$$

- 2) Solve the integral equations (known as Gelfand-Levitan-Marchenko equations) for its unknown kernels $A_1(x, y)$ and $A_2(x, y)$:

$$A_1(x, y) + \int_{-y}^x A_2(x, s) \rho(y+s) ds = 0$$

$$A_2(x, y) + \rho(x+y) + \int_{-y}^x A_1(x, s) \rho(y+s) ds = 0$$

- 3) Compute the potential function $q(x)$ through

$$q(x) = 2A_2(x, x)$$

- 4) By inverting equation (6), compute

$$\frac{L(x)}{C(x)} = \frac{L(x_s)}{C(x_s)} \exp\left(4 \int_{x_s}^x q(s) ds\right)$$

In practice, the integral equations have to be solved numerically, by discretizing the kernels $A_1(x, y)$ and $A_2(x, y)$ over a grid in the x - y plane. By choosing the origin of the x -axis such that $x_s > 0$, the potential $q(x) = 0$ for $x < 0$. It is then sufficient to compute the kernels $A_1(x, y)$ and $A_2(x, y)$ in the region $x \geq |y|$. See [6], [7] for the details about the numerical solution of the integral equations.

III. SIMULATION STUDY

In this section, results of simulation will be presented to confirm the validity of the method presented in this paper for characteristic impedance monitoring. The first step is to implement a numerical simulator generating the reflection coefficient $r(k)$ from the specified profiles $L(z)$ and $C(z)$ of a transmission line.

A. Transmission line simulator

Going back to the z -coordinate as used in the telegrapher's equations (1), let

$$Z(k, z) = \frac{V(k, z)}{I(k, z)} \quad (17)$$

be the apparent impedance at the point z . It is then straightforward to check that the telegrapher's equations (1) imply that $Z(k, z)$ satisfies the Riccati equation

$$\frac{\partial}{\partial z} Z(k, z) = jkL(z) - jkC(z)Z^2(k, z)$$

After the Liouville transformation (2), and by noting $Z(k, z(x))$ as $Z(k, x)$, this equation becomes

$$\frac{\partial}{\partial x} Z(k, x) = jkZ_0(x) - jkZ_0^{-1}(x)Z^2(k, x) \quad (18)$$

where $Z_0(x)$ is the characteristic impedance as defined in (4).

For a given value of k , by initializing $Z(k, x)$ with the matched load at the right end, namely

$$Z(k, x_L) = Z_L = Z_0(x_L)$$

equation (18) can be solved for $x < x_L$. In particular, the value $Z(k, x_s)$ at the left end of the transmission line is computed.

Following Figure 1, the voltage $V(k, x_s)$ at the left end of the transmission line is then computed as

$$\begin{aligned} V(k, x_s) &= \frac{Z(k, x_s)}{Z_s + Z(k, x_s)} V_s(k) \\ &= \frac{Z(k, x_s)}{Z_0(x_s) + Z(k, x_s)} V_0(k) \exp(jkx_s) \end{aligned}$$

The incident voltage wave $V_i(k)$ is known from the voltage source. The reflected wave is then deduced as

$$V_r(k) = V(k, x_s) \exp(jkx_s) - V_i(k) \exp(2jkx_s)$$

The computation of the reflection coefficient $r(k)$ following (15) then leads to

$$r(k) = -\frac{Z(k, x_s) - Z_0(x_s)}{Z(k, x_s) + Z_0(x_s)} \exp(2jkx_s) \quad (19)$$

It then appears that the main computation of the simulator consists of the solution of the Riccati equation (18) for the value of the apparent impedance $Z(k, x_s)$. This computation is repeated with different values of k to cover a sufficiently large spectrum.

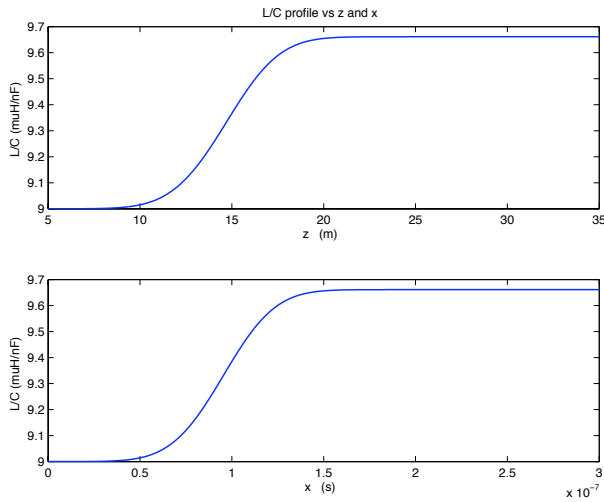


Fig. 2. Simulated smoothly increasing L/C profile.

B. Simulation results

For the first example, a smoothly increasing $L(z)$ profile is simulated. The capacitance is kept to a constant value $C = 0.1\text{nF/M}$, and the corresponding ratio L/C is depicted in Figure 2, in both z and x coordinates. The simulated reflection coefficient $r(k)$ (modulus and phase) is shown in Figure 3. The L/C profile computed through the inverse scattering transform is compared to the original simulated profile in Figure (4).

Remark that the inverse scattering transform computes the ratio L/C as a function of x . In practice it would be more useful to inspect the ratio as a function of z , the true spatial coordinate of the transmission line. Like all reflectometry methods, the information obtained by observing incident and reflected waves is related to the wave propagation time x . Without knowing the wave propagation velocity (varying along the line in the considered case), it is impossible to convert the result from x to z . However, for moderate variations of the ratio L/C (under the soft fault assumption), the two profiles in x and in z are similar, as shown in Figure 2 for the considered example. It is thus practically reasonable to assume a constant wave propagation velocity to convert the computed L/C ratio to the z -coordinate.

For the second example, a hump-shaped L/C profile is simulated, as illustrated in Figure 5. The simulated reflection coefficient is plotted in Figure 6 (in solid line), and the L/C profile computed by inverse scattering in Figure 7. Again the simulated L/C profile is correctly retrieved by the inverse scattering transform.

Up to now the computations have been made in this paper under the assumption of perfect model and noise-free measurement. To evaluate the robustness of the method to random measurement uncertainties, noises can be added in the simulation study. As in practice the voltage $V(k, x_s)$ is measured with an instrument, it may be corrupted by an

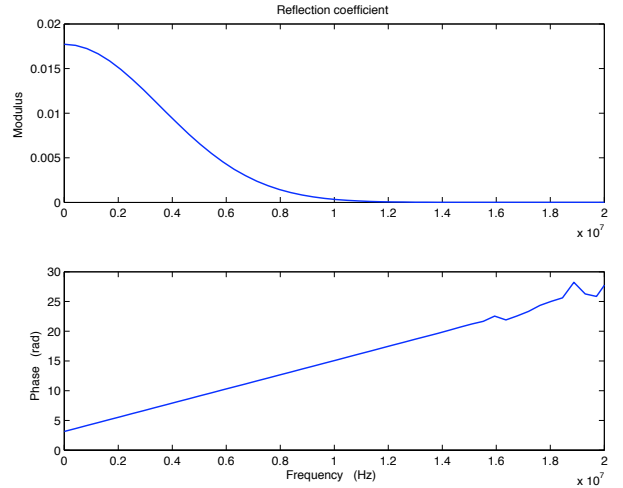


Fig. 3. Simulated reflection coefficient for the smoothly increasing L/C profile.

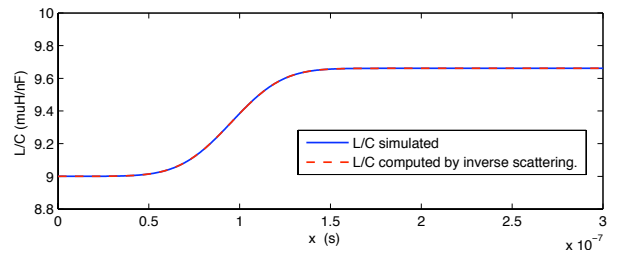


Fig. 4. The smoothly increasing L/C profile computed by inverse scattering and compared to the simulated profile. The two curves may not be distinguishable if printed in black and white.

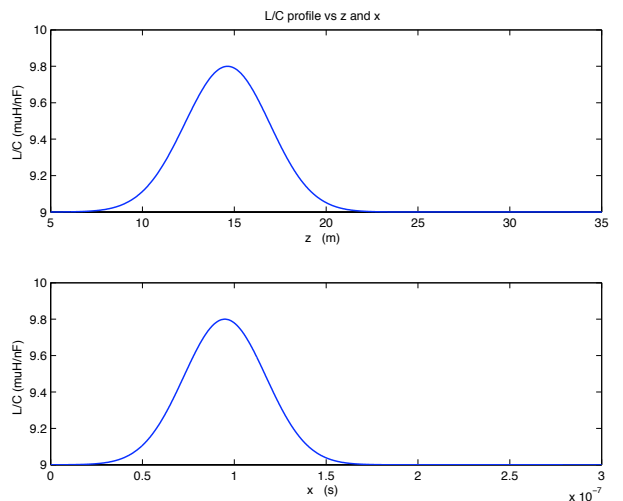


Fig. 5. Simulated hump-shaped L/C profile.

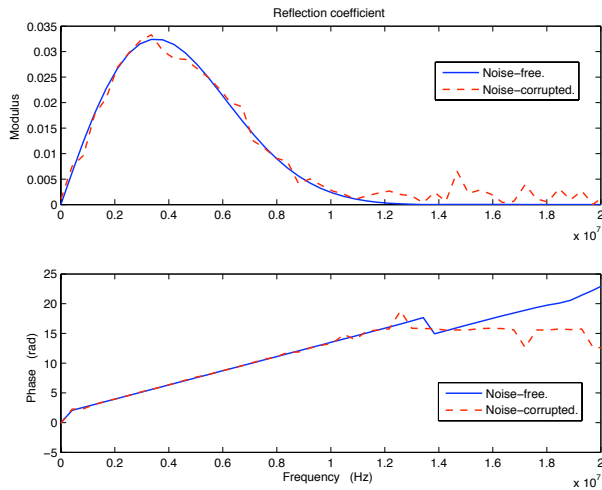


Fig. 6. Simulated reflection coefficients for the hump-shaped L/C profile, the noise-free case in solid line, and the noise-corrupted case in dashed line.

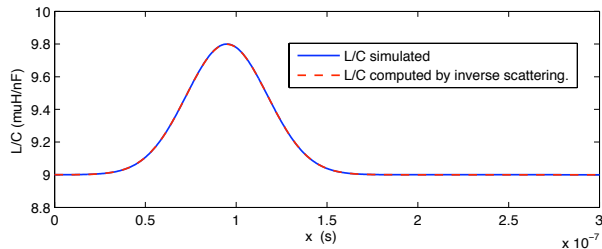


Fig. 7. The hump-shaped L/C profile computed by inverse scattering and compared to the simulated profile. The two curves may not be distinguishable if printed in black and white.

additive noise, say $e(k)$. Consequently, an extra term

$$-2 \frac{e(k)}{V_s(k)} \exp(2jkx_s)$$

is added to equation (19), where $V_s(k)$ is the voltage of the source connected to the transmission line. For the same noise $e(k)$, the more powerful is the voltage source, the less important is the influence of the noise to the measured reflection coefficient.

The second simulation example is then repeated by adding a Gaussian noise $e(k)$ with its standard deviation equal to 0.1% of the amplitude of the voltage source $V_s(k)$. The resulting simulated reflection coefficient (in dashed line), compared to the noise-free coefficient (in solid line), is shown in Figure 6. Though the noise is small compared to the voltage source, it disturbs considerably the reflection coefficient: the standard deviation of the noise added to $r(k)$ is equal to about 6.2% of the maximum absolute value of the simulated $r(k)$. The impact of the noise depends on the absolute values of the reflection coefficient.

The hump-shaped L/C profile is then computed by inverse scattering from the noise-corrupted reflection coefficient. The result is illustrated in Figure 8. Though the reflection coefficient has been considerably corrupted, the inverse scattering transform is still capable of retrieving reasonably the L/C profile.

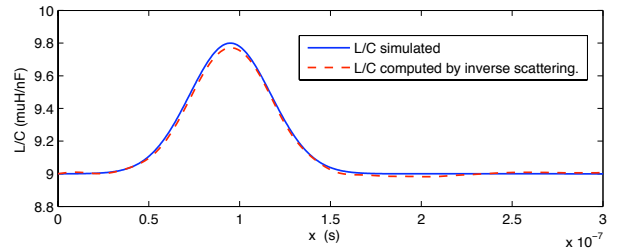


Fig. 8. The hump-shaped L/C profile computed by inverse scattering from noise-corrupted reflection coefficient.

IV. CONCLUSION

Though the theoretic basis for the inverse scattering problem of electric transmission lines has been founded about a quarter of a century ago, there has been a gap between this theoretic result and its practical application. By clarifying the relationship between the reflection coefficient measured in usual engineering practices and the mathematical object of the same name defined in the scattering theory, this paper constitutes an attempt to fill this gap. Moreover, the simulation studies reported in this paper confirm the feasibility of this approach.

Before closing this paper, let us make a comment about lossy transmission lines. As shown by Jaulent in [4], after the transformations used in this paper, an extra nonlinear variable change transforms the telegrapher's equations for lossy transmission lines to a pair of Zakharov-Shabat equations similar to equations (5), but with two distinct potential functions $q^+(x)$ and $q^-(x)$ in the two equations. Compared to the lossless case, the number of unknowns is doubled. Similar Gelfand-Levitan-Marchenko integral equations can be established in this case. To solve them for the doubled unknowns, both the left and right reflection coefficients are required. To our knowledge, no practical implementation of such an algorithm has been reported. Another possible difficulty is related to the nonlinear variable change, which may cause numerically ill-conditioned computations. Further studies are necessary to complete the solution to this practically important problem.

REFERENCES

- [1] P. Smith, C. Furse, and J. Gunther, "Analysis of spread spectrum time domain reflectometry for wire fault location," *IEEE Sensors Journal*, vol. 5, no. 6, pp. 1469–1478, December 2005.
- [2] F. Auzanneau, M. Olivas, and N. Ravot, "A simple and accurate model for wire diagnosis using reflectometry," in *PIERS Proceedings*, August 2007.
- [3] L. A. Griffiths, R. Parakh, C. Furse, and B. Baker, "The invisible fray: A critical analysis of the use of reflectometry for fray location," *IEEE Sensors Journal*, vol. 6, no. 3, pp. 697–706, June 2006.
- [4] M. Jaulent, "The inverse scattering problem for LCRG transmission lines," *Journal of Mathematical Physics*, vol. 23, no. 12, pp. 2286–2290, December 1982.
- [5] G. L. Lamb, *Elements of Soliton Theory*. New York: John Wiley & Sons, 1980.
- [6] P. V. Frangos and D. L. Jaggard, "A numerical solution to the zakharov-shabat inverse scattering problem," *IEEE transactions on antennas and propagation*, vol. 39, no. 1, pp. 74–79, 1991.
- [7] G. Xiao and K. Yashiro, "An efficient algorithm for solving zakharov-shabat inverse scattering problem," *IEEE Transactions on Antennas and Propagation*, vol. 50, no. 6, pp. 807–811, June 2002.